Chemical Physics 375 (2010) 503–507

Contents lists available at ScienceDirect

Chemical Physics

journal homepage: www.elsevier.com/locate/chemphys

Lateral electron transport in monolayers of short chains at interfaces: A Monte Carlo study

Christopher B. George [a,*], Igal Szleifer [a,b], Mark A. Ratner [a]

[a] Department of Chemistry, Northwestern University, Evanston, IL 60208, United States
[b] Department of Biomedical Engineering, Northwestern University, Evanston, IL 60208, United States

ARTICLE INFO

Article history:
Received 16 February 2010
In final form 20 April 2010
Available online 1 June 2010

Keywords:
Melting transition
Static percolation
Electron transfer
Redox-active monolayer

ABSTRACT

Using Monte Carlo simulations, we study lateral electronic diffusion in dense monolayers composed of a mixture of redox-active and redox-passive chains tethered to a surface. Two charge transport mechanisms are considered: the physical diffusion of electroactive chains and electron hopping between redox-active sites. Results indicate that by varying the monolayer density, the mole fraction of electroactive chains, and the electron hopping range, the dominant charge transport mechanism can be changed. For high density monolayers in a semi-crystalline phase, electron diffusion proceeds via electron hopping almost exclusively, leading to static percolation behavior. In fluid monolayers, the diffusion of chains may contribute more to the overall electronic diffusion, reducing the observed static percolation effects.

1. Introduction

The incorporation of redox-active moieties into two-dimensional (2D) molecular assemblies has been the subject of a number of studies in recent years. Technological applications in areas such as solar energy conversion [1,2], sensors [3], and molecular electronics [4–7] have fueled researchers' interest in understanding how electrons move across 2D supramolecular systems. Such systems include self-assembled monolayers [1,2,8,9], Langmuir monolayers [10–13], and bilayers [14].

The dominant mechanisms controlling lateral charge transport have been explored both theoretically [15,16] and experimentally [10,11]. In systems containing both reduced and oxidized species, the Dahms–Ruff equation predicts that two modes of motion are primarily responsible for the diffusion of electrons: physical displacement of redox centers and hopping of electrons between oxidized and reduced sites [17–19]. Blauch and Saveant have explored the relationship between the two mechanisms in detail and shown that the electronic diffusion exhibits percolation behavior when the rate of electron hopping contributes more to lateral charge transport than the physical motion of redox sites [15]. In this case, the electrons' lateral diffusion remains very low below a critical concentration of electroactive species because electrons are confined to hop within clusters of redox-active molecules distributed throughout the system. For concentrations larger than the critical threshold (percolation threshold), a cluster of redox-active molecules exists that spans the entire system and permits long-range electronic diffusion. This percolation behavior is progressively washed out as the lateral mobility of electroactive sites increases. Experimental studies of Langmuir monolayers as well as self-assembled monolayers have confirmed the percolation behavior [1,2,11], and the change in the lateral charge transport mechanism from redox-site diffusion to electron hopping has been observed in a Langmuir monolayer of electroactive molecules [10].

The objective of this study is to understand how the dominant mechanism of lateral charge transport changes in monolayers of surfactants at interfaces. Of particular interest is the role that the monolayer's phase behavior has on the dominant charge transport mechanism. Langmuir monolayers composed of amphiphilic molecules exhibit a number of different condensed phases characterized by positional ordering, collective tilt behavior, and backbone ordering [20]. The dynamical behavior of molecules within the monolayer may be dramatically affected by phase transitions, especially those involving a change in the positional ordering such as a melting transition [21–23].

Using a coarse-grained model to represent monolayers of mobile, electroactive chains, we probe the effects of monolayer density, mole fraction of electroactive molecules, and electron hopping range on the overall electron diffusion rates. Monolayer densities are chosen below and above the melting transition to explore the role that physical motion plays in lateral charge transport. Results indicate that a crossover in the electronic diffusion mechanism occurs in fluid monolayers: lateral chain diffusion contributes more to electronic diffusion when there is a low surface concentration of electroactive chains while electron hopping dominates at higher surface concentrations. The concentration at which the crossover occurs depends on the electron hopping range. For

* Corresponding author.
E-mail address: c-george@u.northwestern.edu (C.B. George).

0301-0104/$ - see front matter © 2010 Elsevier B.V. All rights reserved.
doi:10.1016/j.chemphys.2010.04.041

semi-crystalline monolayers, no crossover is evident due to limited chain diffusion.

2. Computational method

2.1. Surfactant model

Surfactant molecules are represented by chains of four Lennard-Jones monomers connected by springs (Fig. 1) where the Lennard-Jones potentials are truncated and shifted to be purely repulsive:

$$V_{LJ}(r_{ij}) = \begin{cases} 4\varepsilon_{LJ}\left[\left(\frac{\sigma}{r_{ij}}\right)^{12} - \left(\frac{\sigma}{r_{ij}}\right)^{6}\right] - 4\varepsilon_{LJ}\left[\left(\frac{\sigma}{r_c}\right)^{12} - \left(\frac{\sigma}{r_c}\right)^{6}\right]; & \text{for } r_{ij} \leqslant r_c, \\ 0: & \text{for } r_{ij} > r_c. \end{cases} \quad (1)$$

The cutoff radius is $r_c = 2^{1/6}\sigma$ with σ representing the range of the Lennard-Jones potential. The "hardness" of the repulsive potential is given by ε_{LJ}, and the distance between monomers is r_{ij}. Springs connecting neighboring monomers are described by a finitely extensible nonlinear elastic (FENE) potential:

$$V_s(d) = \begin{cases} -\frac{k_s}{2}d_s^2 \ln\left[1 - \frac{(d-d_0)^2}{d_s^2}\right], & \text{for } |d-d_0| < d_s \\ \infty & \text{for } |d-d_0| > d_s. \end{cases} \quad (2)$$

Here, d is the distance between neighboring monomers, d_0 is the equilibrium bond length, d_s is the maximum spring extension, and k_s is the spring constant. The angular potential has the form:

$$V_A(\theta) = k_A(1 + \cos\theta), \quad (3)$$

where k_A is the bond angle force constant and θ is the angle between three successive monomers (Fig. 1). Monomers are permitted to translate in any direction with the restrictions that one monomer (defined as the head monomer) is confined to translate in the $z = 0$ plane while the rest must remain above the xy plane.

The model in this study is similar to previous models used to examine the phase behavior of Langmuir monolayers [24–28]. As in earlier works, we define parameters as $d_s = 0.2$, $d_0 = 0.7$, $k_s = 100$, and $k_A = 10$ [24–28]. These parameter values prevent chains from intersecting and becoming tangled. Rough estimates of the length scale in physical units have yielded $\sigma \approx 5$ Å [26]. This estimate is obtained by assuming that each model chain represents an alkyl chain with a single monomer representing 2–5 methyl groups.

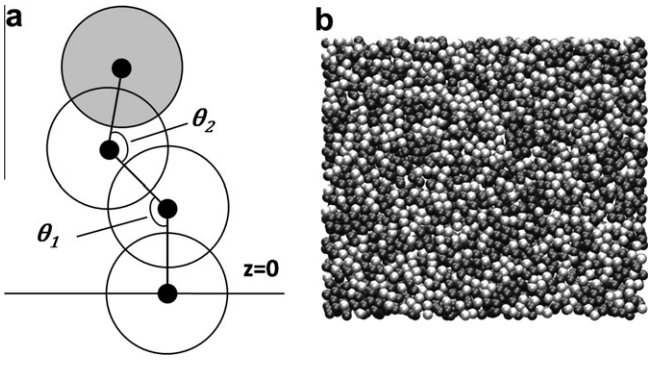

Fig. 1. (a) Four Lennard-Jones monomers connected by springs constitute the model used to describe electroactive chains. Angular potentials are calculated from θ_1 and θ_2. The head monomer is constrained to translate in the xy plane while the remaining monomers may move above the plane. The shaded monomer represents the electroactive moiety. (b) A snapshot of an equilibrated monolayer composed of a mix of chains with redox-active (light gray monomers) and redox-passive (black monomers) sites.

While simulations based on the Metropolis Monte Carlo algorithm technically have no physical time scale, the use of physically reasonable moves has permitted the study of diffusive motion in amphiphilic monolayers [23] and bilayers [29] using Monte Carlo techniques. As described by Wang and Frenkel [29] the time scale of a Monte Carlo step may be estimated by comparing lateral diffusion coefficients determined from experiment and simulation. Lateral diffusion coefficients can be computed from simulation via the lateral mean squared displacement (MSD). The relationship between the lateral diffusion coefficient and two-dimensional MSD is:

$$D_{xy} = \frac{\left\langle (r_{xy}(t) - r_{xy}(0))^2 \right\rangle}{4t}. \quad (4)$$

Here t represents time. Using the previously defined length scale ($\sigma \approx 5$ Å), a comparison with an experimental diffusion coefficient [12,30–32] of $\sim 10^{-7}$–10^{-8} cm^2/s results in one Monte Carlo step (MCS) corresponding to $\sim 10^{-12}$ s. Both experimental and theoretical diffusion coefficients were determined for Langmuir monolayers in the fluid phase.

2.2. Electron hopping

Electron transfer occurs in the monolayer between electroactive chains that are randomly distributed. The fourth monomer (on the opposite side of the chain as the head monomer, see Fig. 1) is the redox-active site. We assume the rate of electron transfer between two electroactive sites depends exponentially on the distance separating the sites:

$$k(r) = c_0 e^{-\beta r}. \quad (5)$$

The decay factor β describes the sensitivity of electron transfer to distance. Experimental values range from $\beta = 0.5$–2.5 Å^{-1} depending on the medium through which the transfer occurs, corresponding to $\beta = 2.5$–12.5 σ^{-1} [16]. The parameter c_0 gives the rate of the fastest possible electron transfer for a particular system; we define $c_0 = 10^{13}$ s^{-1} which is equivalent to a rate of $\frac{10}{1\ \mathrm{MCS}}$.

To determine the average frequency with which electron hops should occur, the overall rate is computed by summing the rates of all possible hops:

$$k_{tot} = \sum_{i=1}^{n-1} k(r_i). \quad (6)$$

Here n is the total number of redox-active sites and $k(r_i)$ is defined by Eq. (5). For each electron hop, a redox-active destination site is selected with probability $k(r_i)/k_{tot}$. The frequency of electron hops is calculated at the beginning of the simulation and updated after each subsequent hopping event.

Every simulation contains multiple electrons that move independently of one another. Electron hops are energetically neutral, and the role of counterions as well as any other electrostatic effects have been disregarded.

2.3. Simulation details

Off-lattice Metropolis Monte Carlo simulations are performed in the canonical ensemble with 1024 chains in a rectangular simulation box. The simulation cell has periodic boundary conditions and an aspect ratio ($L_y/L_x = \sqrt{3}/2$) designed to accommodate hexagonal packing. All simulations are performed with the reduced temperature $T^* = \frac{T}{\varepsilon} = 1$. Several densities ($\rho\sigma^2 = \rho^* = 0.6, 0.75, 0.9$) are studied with a range of β values ($\beta = 4.0$–$12\ \ \sigma^{-1}$) and mole fractions of redox-active chains ($X = 0.1$–1.0). Simulations are equilibrated for a period of 10^6 Monte Carlo steps where one MCS represents 4096 attempted monomer moves, corresponding to

one attempt per monomer on average. Electron hopping moves are performed with frequencies defined by Eq. (6). After equilibration, simulations are run for at least 10^5 MCS to obtain linear behavior of the electrons' average mean squared displacement as a function of time. This permits calculation of the electrons' lateral diffusion coefficient from Eq. (4).

Additional runs are performed for a wider range of densities ($\rho^* = 0.5$–1.05) to characterize the monolayer's phase behavior. In these simulations, no electron transfer moves are performed. These run are equilibrated for 5×10^5 MCS with an additional 5×10^5 MCS performed for data collection.

3. Results and discussion

3.1. Melting transition

As a monolayer becomes more dense, chains are forced to pack closer together until they begin to exhibit well defined hexagonal order. This order–disorder transition has been well-studied in purely two-dimensional systems [33], and order parameters have been devised that show when such a transition has occurred. One such order parameter, the bond orientation order parameter, is defined as [33]:

$$\langle |\Psi_6| \rangle = \left\langle \left| \frac{1}{N} \sum_{i}^{N} \frac{1}{n_i} \sum_{j=1}^{n_i} e^{i6\theta_{ij}} \right| \right\rangle. \tag{7}$$

Here, N is the number of particles, n_i is the number of nearest neighbors for particle i, and θ_{ij} is the angle between the line connecting neighboring particles i and j and an arbitrary axis. Fig. 2 shows values of the head monomer's bond orientation order parameter. The jump in $\langle |\Psi_6| \rangle$ at $\rho^* = 0.76$ indicates that a liquid–solid transition has taken place with increased hexagonal packing at higher densities.

The effect of the order–disorder transition on the dynamics of the surfactant molecules within the monolayer is dramatic. Fig. 3 shows the average lateral mean squared displacements of chains within monolayers that have densities below ($\rho^* = 0.60$), very near ($\rho^* = 0.75$), and above ($\rho^* = 0.90$) the melting transition. It is evident that normal diffusion takes place for the two lower densities because the average mean squared displacements vary linearly with time. The steeper slope in the MSD for the monolayer with a density of ($\rho^* = 0.60$) indicates a larger lateral diffusion coefficient compared to the monolayer with ($\rho^* = 0.75$). This is due to increased crowding effects at higher densities. Above the transition,

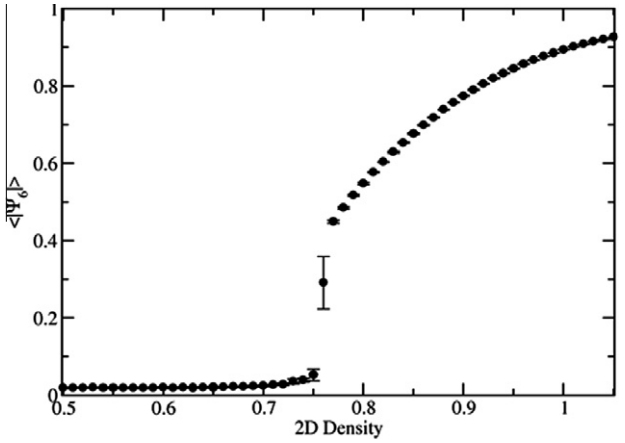

Fig. 2. The bond orientation order parameter $\langle |\Psi_6| \rangle$ as a function of density (in units of σ^{-2}) for the head monomers shows evidence of a melting transition near $\rho^* = 0.76$.

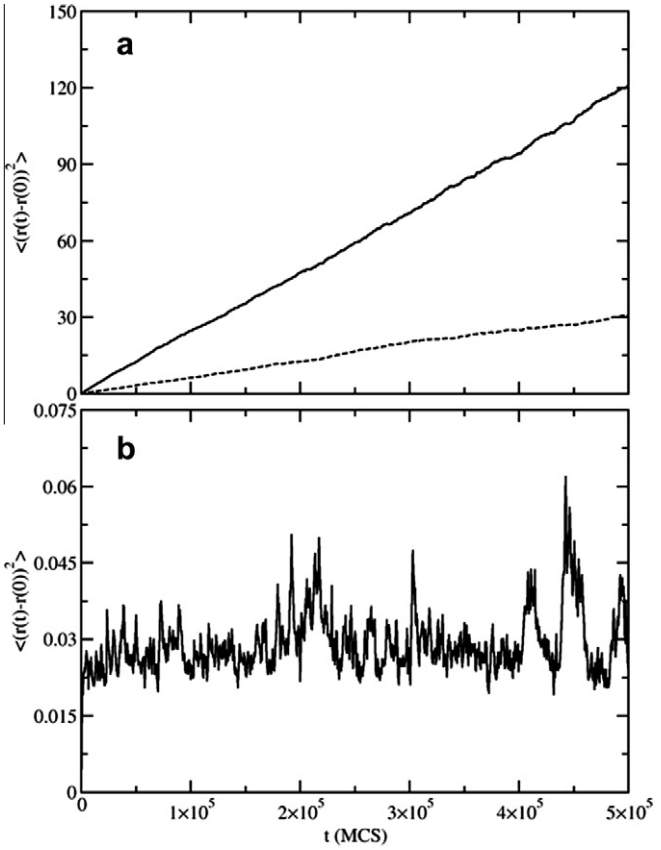

Fig. 3. Mean squared displacements in units of σ^2 vs. time in units of Monte Carlo steps (MCS) for monolayers (a) below ($\rho^* = 0.60$, solid line), near ($\rho^* = 0.75$, dashed line), and (b) above ($\rho^* = 0.90$) the melting transition. Monolayers below and near the transition exhibit normal diffusion with mean squared displacements linearly dependent on time. Above the transition density, monolayers exist in a semi-crystalline state with minimal lateral displacement.

the mean squared displacement is virtually zero. In this case, the Brownian motion of the chains [34] is almost completely constrained by nearest neighbors such that not even single file diffusion can occur [35].

By selecting monolayers in both the fluid and semi-crystalline phases, the effect of the physical diffusion of chains on the lateral charge transport should be apparent. Transport in the high density case will be facilitated only by electron hopping, regardless of the β value or the mole fraction of redox-active chains, while the lower density cases should have a combination of both mechanisms. Controlling monolayer densities independent of the concentration of redox-active sites permits an additional level of control over the charge transport mechanism, in contrast to earlier studies in which the mobilities of redox-active sites were highly dependent on the concentrations of electroactive centers [15].

3.2. Electron diffusion

Lateral diffusion coefficients for the electronic motion are calculated from the slopes of the average electronic mean squared displacements using Eq. (4). Plots of the diffusion coefficients as a function of the mole fraction, X, of redox-active chains are shown in Fig. 4 for simulations with several different β values.

Percolation behavior is evident for monolayers with a density of $\rho^* = 0.90$ for all β values. At low values of X, lateral electron diffusion is minimal. Diffusion coefficients begin to rise linearly with X after a critical concentration is reached (the percolation threshold). At this threshold, one or more clusters of redox-active molecules

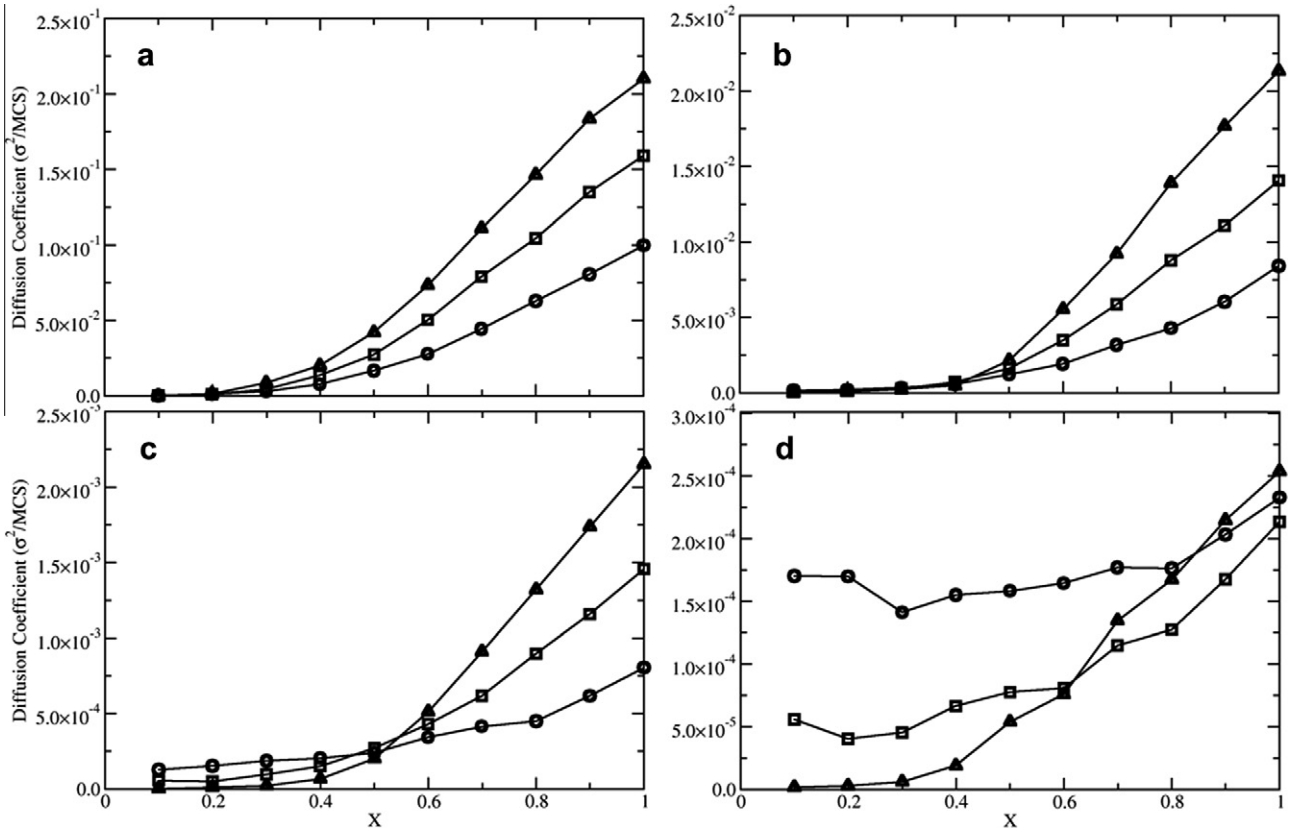

Fig. 4. Electronic diffusion coefficients as a function of the mole fraction of electroactive chains, X, for monolayers with densities of $\rho^* = 0.60$ (circle), $\rho^* = 0.75$ (square), and $\rho^* = 0.90$ (triangle). Points represent simulation results for (a) $\beta = 4.0$, (b) $\beta = 6.0$, (c) $\beta = 8.0$, and (d) $\beta = 10.0$, all in units of σ^{-1}. For $\sigma = 5$ Å, this corresponds to a range of $\beta = 0.8$–2.0 Å^{-1}. Values of β change the relative rate of hopping defined by Eq. (6), changing the relative effect the physical diffusion of chains has on lateral electron transport.

span the monolayer allowing macroscopic charge transport to occur. The triangular lattice formed by the semi-crystalline monolayer has a percolation threshold of 0.5 according to classical percolation theory [36]. This threshold holds true in systems with hopping between nearest neighbors only, but longer range electron hopping shifts the threshold to lower mole fractions because electrons may hop between unconnected clusters [16]. The shift can be seen in simulations with $\beta = 4.0\ \sigma^{-1}$ and $\rho^* = 0.90$ where the critical concentration appears near $X = 0.3$. At higher values of β with the same density, less long-range hopping occurs and the threshold lies closer to the classical percolation threshold of $X = 0.5$.

Percolation behavior begins to be washed out in fluid monolayers due to the physical diffusion of chains, in agreement with results obtained by Blauch and Saveant [15]. As β increases, the relative contribution of chain mobility to the electronic diffusion becomes greater than the contribution of electron hopping. The reason for this is twofold: a rise in β leads to fewer long-range hops as well as less frequent attempted hops. The overall frequency of hops is lower because $k(r) = c_0 e^{-\beta r}$ is smaller for all distances r, lowering the overall hopping rate defined by Eq. (6). The physical diffusion of chains, on the other hand, remains constant, independent of β.

The change in transport mechanism from predominantly electron hopping to a mix of hopping and physical diffusion of chains is most evident for the lower density monolayers with $\beta = 8\sigma^{-1}$ and $\beta = 10\sigma^{-1}$. At the lower mole fractions, the diffusion coefficients vary inversely with the densities of the monolayers. This can only be due to the effects of chain mobility. For two immobile monolayers with identical mole fractions but different densities, the higher density monolayer will have faster electron hopping rates on average because the typical distance between electroactive molecules is less. In mobile systems, the lower density monolayer will have greater chain mobility (as seen in Fig. 3), potentially leading to higher electronic diffusion rates. The rate increase is a result of more frequent hopping due to the reorganization of electroactive clusters as well as transport of charge by the movement of chains. Both processes occur in the fluid monolayers in our simulations, and the relative contribution of each to the overall electronic diffusion may be determined by inspecting the dependence of the diffusion rates on the mole fraction. Diffusion rates that increase with X are a sign of increased electron hopping while rates that are nearly independent of X indicate transport predominantly by chain diffusion.

4. Conclusions

The diffusion of charge in a monolayer composed of redox-active and redox-passive chains has been examined using Monte Carlo simulations. Two main mechanisms for charge transport are observed: electron hopping between electroactive chains and the physical diffusion of redox-active chains. The relative contributions of the two processes to the overall lateral charge transport are found to be dependent on the mole fraction of electroactive chains within the monolayer, the length decay factor β describing long-range electron transfer, and the monolayer density.

Electronic diffusion occurs almost exclusively via the hopping mechanism in semi-crystalline monolayers due to the minimal physical diffusion of chains. Consequently, strong percolation behavior is evident at all β values studied. In fluid monolayers,

the physical diffusion of chains becomes increasingly important in simulations with fewer long-range hops and less frequent hops overall. These conditions occur in simulations with large β values and low surface concentrations of electroactive molecules.

The results underscore the dependence of lateral electron diffusion on the phase behavior of the facilitating monolayer. While previous work has shown that redox-site mobility strongly influences both percolation effects and the lateral charge transport mechanism [15], the present work illustrates how one might manipulate lateral charge transport behavior utilizing the phase behavior of Langmuir monolayers. By compressing a monolayer composed of electroactive and inert molecules beyond the order–disorder transition, it is possible to either raise or lower the rate of lateral charge transport, depending on the ratio of active to passive species. This tunability suggests possible applications controlling electron transfer through biological membranes or mobile monolayers.

Acknowledgements

C.B.G. is supported by a Graduate Research Fellowship from the NSF. This work was supported by the Non-equilibrium Energy Research Center (NERC) which is an Energy Frontier Research Center funded by the US Department of Energy, Office of Science, Office of Basic Energy Sciences under Award No. DE-SC0000989.

References

[1] P. Bonhote, E. Gogniat, S. Tingry, C. Barbe, N. Vlachopoulos, F. Lenzmann, et al., J. Phys. Chem. B 102 (1998) 1498.
[2] N. Papageorgiou, M. Gratzel, O. Enger, D. Bonifazi, F. Diederich, J. Phys. Chem. B 106 (2002) 3813.
[3] A. Bardea, F. Patolsky, A. Dagan, I. Willner, Chemical Communications, vol. 21, Cambridge, UK, 1999.
[4] F.R.F. Fan, J.P. Yang, L.T. Cai, D.W. Price, S.M. Dirk, D.V. Kosynkin, et al., J. Am. Chem. Soc. 124 (2002) 5550.
[5] F.R.F. Fan, R.Y. Lai, J. Cornil, Y. Karzazi, J.L. Bredas, L.T. Cai, et al., J. Am. Chem. Soc. 126 (2004) 2568.
[6] F.R.F. Fan, Y.X. Yao, L.T. Cai, L. Cheng, J.M. Tour, A.J. Bard, J. Am. Chem. Soc. 126 (2004) 4035.
[7] T. Ishida, W. Mizutani, U. Akiba, K. Umemura, A. Inoue, N. Choi, et al., J. Phys. Chem. B 103 (1999) 1686.
[8] B. O'Regan, M. Gratzel, Nature 353 (1991) 737.
[9] S.A. Trammell, T.J. Meyer, J. Phys. Chem. B 103 (1999) 104.
[10] R.J. Forster, T.E. Keyes, R. Majda, J. Phys. Chem. B 104 (2000) 4425.
[11] W.Y. Lee, M. Majda, G. Brezesinski, M. Wittek, D. Mobius, J. Phys. Chem. B 103 (1999) 6950.
[12] D.H. Charych, E.M. Landau, M. Majda, J. Am. Chem. Soc. 113 (1991) 3340.
[13] C.A. Widrig, C.J. Miller, M. Majda, J. Am. Chem. Soc. 110 (1988) 2009.
[14] C.J. Miller, C.A. Widrig, D.H. Charych, M. Majda, J. Phys. Chem. 92 (1988) 1928.
[15] D.N. Blauch, J.M. Saveant, J. Am. Chem. Soc. 114 (1992) 3323.
[16] D.N. Blauch, J.M. Saveant, J. Phys. Chem. 97 (1993) 6444.
[17] I. Ruff, V.J. Friedrich, J. Phys. Chem. 75 (1971) 3297.
[18] I. Ruff, V.J. Friedrich, K. Demeter, K. Csillag, J. Phys. Chem. 75 (1971) 3303.
[19] H. Dahms, J. Phys. Chem. 72 (1968) 362.
[20] V.M. Kaganer, H. Mohwald, P. Dutta, Rev. Mod. Phys. 71 (1999) 779.
[21] B.X. Cui, B.H. Lin, S.A. Rice, J. Chem. Phys. 114 (2001) 9142.
[22] R. Zangi, S.A. Rice, Phys. Rev. E 68 (2003) 061508.
[23] T. Sintes, A. Baumgaertner, Y.K. Levine, Phys. Rev. E 60 (1999) 814.
[24] F.M. Haas, R. Hilfer, J. Chem. Phys. 105 (1996) 3859.
[25] F.M. Haas, R. Hilfer, K. Binder, J. Chem. Phys. 102 (1995) 2960.
[26] F.M. Haas, R. Hilfer, K. Binder, J. Phys. Chem. 100 (1996) 15290.
[27] D. Duchs, F. Schmid, J. Phys.: Condens. Mat. 13 (2001) 4853.
[28] C. Stadler, F. Schmid, J. Chem. Phys. 110 (1999) 9697.
[29] Z.J. Wang, D. Frenkel, J. Chem. Phys. 122 (2005).
[30] M.B. Forstner, J. Kas, D. Martin, Langmuir 17 (2001) 567.
[31] M.R. Alecio, D.E. Golan, W.R. Veatch, R.R. Rando, Proc. Natl. Acad. Sci. USA 79 (1982) 5171.
[32] B. Lindholm-Sethson, J.T. Orr, M. Majda, Langmuir 9 (1993) 2161.
[33] K.J. Strandburg, Rev. Mod. Phys. 60 (1988) 161.
[34] P. Hanggi, F. Marchesoni, Chaos 15 (2005).
[35] P.S. Burada, P. Hanggi, F. Marchesoni, G. Schmid, P. Talkner, ChemPhysChem 10 (2009) 45.
[36] M.F. Sykes, J.W. Essam, J. Math. Phys. 5 (1964) 1117.